Innovative Infrastructure Solutions (2021) 6:65
https://doi.org/10.1007/s41062-020-00447-z

TECHNICAL PAPER

Compressive strength prediction model of high-strength concrete with silica fume by destructive and non-destructive technique

Rahul Biswas[1] · Baboo Rai[1] · Pijush Samui[1]

Received: 18 July 2020 / Accepted: 21 December 2020 / Published online: 12 January 2021

Abstract

The study proposes a new model for estimating the compressive strength of high-strength concrete using destructive and non-destructive testing. The effect of silica fume replacement level and its cementing efficiency factor on compressive strength and ultrasonic pulse velocity (UPV) were experimentally examined. In the present work, the cementing efficiency factor (*k*) for silica fume at different percentage replacement level has been assumed, and at the constant water-to-binder ratio, the compressive strength has been obtained. An exponential relationship is proposed between UPV and compressive strength with a high correlation coefficient. A statistically noteworthy model with a high correlation coefficient $R^2 > 0.90$ is established to study the influence of the variables (%SF and *k*) on UPV results. Finally, the two proposed models were amalgamated to develop a new model to predict the 28-day compressive strength of high-strength concrete. The validity of the model has been verified with the results obtained by different researchers on different types of specimens. The proposed new model is for the strength range of the 40–75 MPa.

Keywords Silica fume · Cementing efficiency factor · Ultrasonic pulse velocity · Compressive strength

Introduction

In the ACI 318 [1], "high-strength concrete (HSC) is that which accomplishes cylinder compressive strength of no less than 41 MPa at 28 days." In the FIP/CIB (1990) [2], HSC is defined as "concrete having a 28-day cylinder compressive strength of 60 MPa." Past research has also shown the cylinder/cube strength ratio to be between about 0.65 and 0.90, although ratios outside that range have also been observed. HSC with low water/binder (w/b) ratio is widely utilized in construction practices during the past decades [3–5]. The high compressive strength of concrete was achieved by decreasing w/b beyond 0.35 which created a rheological constraint, in other words, loss in a slump. Notwithstanding, with the advent of superplasticizers (SP) and the accessibility of different kinds of mineral and compound admixtures and an extraordinary water retarder, concrete of up to 100 MPa compressive strength is now being created economically [2].

The use of silica fume (SF) in concrete is very nearly a routine one these days for getting HSC. As a kind of industrial by-product composed of much silicon dioxide (SiO_2) [6, 7], SF is widely utilized in HSC for many advantages, such as the improvement of compressive strength, elastic modulus, and durability through pozzolanic activity [8, 9]. SF has a detrimental effect on the fresh concrete properties, i.e., the presence of SF in the concrete mix tends to reduce the slump values [10]. The presence of high content of SF in the concrete mix may reduces the fluidity of the cementitious mix due to their high surface area and high adsorption which tends to increase the demand of SP to maintain the workability limits [11, 12].

Earlier researches on the utilization of SF mostly adopted straightforward replacement methods, established earlier for fly ash (FA). Moreover, a few researches [13–15] in the past were also focussed towards utilization of SF in concrete in regards to the proportion of cement replaced through its "cementing efficiency factor" (*k*). The term "efficiency factor" for SF in concrete can be explained as "the number

✉ Baboo Rai
baboo.rai@nitp.ac.in

Rahul Biswas
rahulbiswas.ce16@nitp.ac.in

Pijush Samui
pijush@nitp.ac.in

[1] National Institute of Technology, Patna, Bihar 800005, India

of parts of cement that may be replaced by one part of SF without changing the property studied" [13].

Several researchers [13, 16–20] in the past modified the water-to-cement (w/c) ratio law proposed by Feret, 1896 [21], Bolomey [22], and Abram's [23] to gauge the efficiency of different Supplementary Cementitious Materials (SCM). However, Abram's or Bolomey's w/c ratio law is not directly applicable to concrete containing other SCMs like FA or SF. Thus the above laws require necessary modifications based on experimental research. Smith [16] was the first to modify Abram's law to recommend a justified model for the w/c ratio by introducing a "FA cementing efficiency factor" (k). To assess the k factor, Smith [16] used compressive strength as a basis for estimation of the k value. A similar type of model has been proposed by other researchers by either modifying Abram's law or Bolomey equation [14, 16, 18, 24, 25].

Babu and Prakash [25] suggested two efficiency factors: one of which is a general factor independent of the replacement ratio of SF and the second one depends on the replacement ratio. The overall efficiency was the multiplication of these two factors. The k value for SF in the literature has ranged from 2 to 4 by Loland [26] and 3 by Fagerlund [27]. Jahren [17] ranged the value from 1to 4 depending upon the dosage of SF on the strength ratios. Malathy and Subramanian [28] reported that the k factor for SF increases up to replacement ratio of 10%. In some of the recent studies [29–32], the strength and durability properties of concrete made with some cement–replacement ratios by different SCMs were examined. Besides, alternative k values of different SCMs were estimated. In one study [31] while analysing the test results, the cementing efficiency factor concept was extended to apply to the combined effects of SF and nanosilica (NS) on the sulphate and chloride resistance of concrete, and the synergistic factor was employed to quantify the synergistic effect of SF and NS.

Non-destructive ultrasonic pulse velocity (UPV) testing is currently the most frequently used to examine the mechanical properties and integrity of concrete structures. There have been several reports regarding the impact of parameters on the UPV [33, 34]. Previous studies have predicted compressive strength according to the UPV. An extensive review of their contributions has been undertaken by a few authors [35, 36]. The application of UPV to the non-destructive evaluation of normal strength concrete ($\leq$41 MPa) quality has been widely investigated for decades [37]. Even though there have been many research attempts that intended to evaluate the strength of HSC, there is yet insufficient experimental data for evaluating the concrete compressive strength that is stronger than 40 MPa.

Due to its ease and applicability, the vast majority of the methodologies for evaluating the concrete compressive strength are commonly based on the statistical regression method. This is broadly utilized because it can get a basic, deterministic equation from the tested data. Past investigations [30, 38–41] have called attention to that utilizing the multiple linear regression method can give a progressively precise and reliable prediction of the concrete compressive strength.

The method for predicting cementing efficiency factors results in relatively high uncertainties. From the review of the literature, it can be seen that there was no standardized relationship used to assess the k value. The aim of this research includes a comprehensive examination of the effect of SF on the mechanical properties of concrete at different k values. All the previous researches [25] in estimating the k factor of SF have been built on the strength prediction of concrete at different w/b ratio for different percentage replacement of SF. In the present work, the k factor for SF at different percentage replacement level has been assumed, and at the constant w/b ratio, the compressive strength has been obtained. In addition, a non-destructive methodology in light of UPV measurements is utilized to evaluate the pulse velocity of HSC. The study further proposes a new model for estimating the compressive strength of HSC using the destructive and non-destructive test.

Experimental programme

Materials

In this study, the cement used was ordinary portland cement (OPC) of 43 grade (IS: 8112-1989) [42]. SF was used in its dry densified form. It contains 91.8% of amorphous glassy silicon dioxide in the form of microscopic spherical particles. The average diameter of these particles is in the range of 0.10–0.15 micrometre having a specific gravity of 2.2. Table 1 presents the physical properties and the chemical composition of both the cementitious materials.

The coarse aggregate used was the crushed stone from Pakur sieved to obtain a 20 mm maximum size. After grading, the aggregate was dried under laboratory conditions. The fineness modulus test and sieve analysis were done in accordance with IS 383-2016 [43]. The grading of fine aggregate according to IS 383-2016 confirmed to zone 3 with a fineness modulus of 2.6. FM is the sum of the total percentages retained on each specified sieve divided by 100. ASTM C 33 requires the FM of fine aggregate to be between 2.3 and 3.1. The higher the FM, the coarser the aggregate. Further, ASTM C 33 also states that for HSC, coarse sand with an FM around 3.0 produces concrete with the best workability and highest compressive strength. The water absorption and specific gravity of the fine and coarse aggregates were 1.35% and 2.66 and 0.70% and 2.86, respectively. For this analysis, a superplasticizer based on polycarboxylic

Table 1 Physical and chemical properties of OPC and SF

	OPC	SF
Physical properties		
Specific gravity	3.15	2.21
Specific surface area (m^2/g)	0.225	19.4
Bulk density (kg/m^3)	–	616
Fineness (retained on 90-µm sieve)	3.5	–
Normal consistency	30%	–
Retained on 45-µm sieve	–	1.13%
Pozzolanic activity index (7 d)	–	132%
Chemical properties		
SiO_2	21.20	91.8
Al_2O_3	5.35	0.6
Fe_2O_3	3.40	1.7
MgO	1.44	0.3
Na_2O	–	0.1
K_2O	–	0.8
CaO	63.95	–
C_3S	51.46	–
C_2S	22.00	–
C_3A	6.42	–
C_4AF	10.35	–

ether with an inbuilt viscosity modifying agent (VMA) with the brand name MasterGlenium SKY 8630/8632 was used. The specific gravity of chemical admixture was 1.08.

Mix proportioning

Thirty-five mixes with partial replacement of cement with SF were prepared. Cube specimens of M60 grade concrete with seven different weight percentages of SF (2%, 4%, 6%, 8%, 10% 12%, and 15%) were cast at different k factor for SF in the concrete mix. The Smith model shown in Eq. 1 has been used in forecasting the actual cement content required at different *k* for SF concrete.

$$\frac{w}{c} = \frac{w}{c_1 + k \times \mathrm{SF}} \quad (1)$$

where w is water content, c is cement content of control concrete, c_1 is cement content of SF concrete, SF is silica fume content, and k is cementing efficiency factor. A "k" value approaching one means that the addition is equivalent to cement. To find the effect of cementing efficiency of SF in concrete, properties like workability, compressive strength, and UPV have been evaluated following the Bureau of Indian Standard Specifications [44]. For this purpose, the k value of SF was assumed and varied from 1 to 5 [45], while w/b ratio was fixed at 0.36. The dosage of chemical admixture was set at 2.2% by weight of cement to obtain the required workability of HSC mixes. The Indian standard mix proportioning guideline as mentioned in IS 10,262:2009 [46] has been used for mix proportioning. The absolute volume of the HSC mix is 1 m^3. The viscosity modifier polymer present in SP becomes active after 3–4 min of continuous mixing. Hence, volume of air which is in the range of 8–10 L in 1 m^3 concrete is removed by increasing the mixing time. Table 2 presents the mix proportions of 1 m^3 concrete.

Test methods

The HSC mixes were designed for non-pumpable concrete with degree of workability medium. According to IS 456-2000, the slump value for medium degree of workability ranges between 50 and 100 mm. The workability of fresh concrete is most commonly measured by slump test in accordance with IS 1199-1959 [47].

A digital compression testing machine of 2000 kN capacity was used for measuring the compressive strength of test specimens. Compressive strength was measured at 7, 14, and 28 days on 150 mm cubes following the norms documented in Indian Standard IS 516-1959 [48]. Three cubes were tested for each age, and average values were obtained. In the present experimental investigation, it was observed that at the age of 28 days, the strength of concrete containing SF was more than that of control concrete which indicated that the initial reaction of pozzolanic material was completed well before 28 days to correlate the cementing efficiency of SF in HSC. Further, as the aim of the research was to gauge the cementing efficiency of SF at 28 days hence 60- or 90-day strength was not considered.

After mixing in a pan mixer, cube specimens for compressive strength testing were cast into mould were compacted by means a vibrating table. After 24 h, the specimens were demoulded and were cured in a water tank at a room temperature until the day of testing.

UPV tests were conducted in conjunction with IS 13311(Part-1) 1992 [49] at 28 days on concrete cube specimens. To generate pulse velocity along the concrete cube specimens, electrical transducers with a frequency range, 20–100 kHz, were used. Pulses are not transmitted through large air voids present in the concrete sample. Therefore, if such a void lies directly in the pulse path then the time taken by the pulse will be more and hence lower velocity will be recorded. A jelly or grease is commonly used as a viscous material, which also acts as a coupling agent to ensure that the vibrational energy passes through the test samples and can be detected by the receiving transducer.

Table 2 Concrete mix proportions

Mix no.	Cement (kg)	w/b	*k**	%SF	SF (kg)	CA (kg)	FA (kg)	SP (kg)	Water (kg)
Control mix	390.0	0.36	–	0	0	1050	866	8.58	140
1	382.2	0.36	1	2	7.8	1049	865	8.58	140
2	374.4	0.36	1	4	15.6	1046	863	8.58	140
3	366.6	0.36	1	6	23.4	1043	860	8.58	140
4	358.8	0.36	1	8	31.2	1041	858	8.58	140
5	351.0	0.36	1	10	39.0	1038	856	8.58	140
6	343.2	0.36	1	12	46.8	1042	865	8.58	140
7	331.5	0.36	1	15	58.5	1039	862	8.58	140
8	374.4	0.36	2	2	7.8	1111	880	8.58	140
9	358.8	0.36	2	4	15.6	1062	881	8.58	140
10	343.2	0.36	2	6	23.4	1062	881	8.58	140
11	327.6	0.36	2	8	31.2	1064	882	8.58	140
12	312.0	0.36	2	10	39.0	1065	883	8.58	140
13	296.4	0.36	2	12	46.8	1080	886	8.58	140
14	273.0	0.36	2	15	58.5	1085	890	8.58	140
15	366.6	0.36	3	2	7.8	1063	882	8.58	140
16	343.2	0.36	3	4	15.6	1068	886	8.58	140
17	319.8	0.36	3	6	23.4	1074	891	8.58	140
18	296.4	0.36	3	8	31.2	1079	895	8.58	140
19	273.0	0.36	3	10	39.0	1083	898	8.58	140
20	249.6	0.36	3	12	46.8	1091	900	8.58	140
21	214.5	0.36	3	15	58.5	1100	905	8.58	140
22	358.8	0.36	4	2	7.8	1067	885	8.58	140
23	327.6	0.36	4	4	15.6	1076	893	8.58	140
24	296.4	0.36	4	6	23.4	1084	900	8.58	140
25	265.2	0.36	4	8	31.2	1093	907	8.58	140
26	234.0	0.36	4	10	39.0	1103	915	8.58	140
27	202.8	0.36	4	12	46.8	1114	912	8.58	140
28	156.0	0.36	4	15	58.5	1126	922	8.58	140
29	351.0	0.36	5	2	7.8	1071	889	8.58	140
30	312.0	0.36	5	4	15.6	1084	899	8.58	140
31	273.0	0.36	5	6	23.4	1096	910	8.58	140
32	234.0	0.36	5	8	31.2	1113	924	8.58	140
33	195.0	0.36	5	10	39.0	1122	930	8.58	140
34	156.0	0.36	5	12	46.8	1135	930	8.58	140
35	97.5	0.36	5	15	58.5	1153	944	8.58	140

**k* Efficiency factor of silica fume

Results and discussion

Workability

Densified SF has been used as one of the binders in the mix whose fineness was 100 times more than cement. To avoid flocculation during secondary hydration, the solid present in the chemical admixture should be high. Role of admixture depends upon its solid content and water. The solid content in the admixture was on the lower side, 25% of the total mass. So the dosage of chemical admixture increased up to 2.2% for required de-flocculation of the binder particles and to achieve the desired workability.

It was also observed that at higher percentage replacement level of SF, the dosage of HRWR needs to be increased to maintain w/b ratio to retain the slump and to achieve target compressive strength. However, in the present work as the desired workability was achieved, there was no requirement to increase the superplasticizers dosage to regulate the slump of the mixtures. Moreover, increase in dosage of SP will also increase the surplus water present in SP after some transit time, i.e., time of start of secondary reaction, which may create adverse effect on physical and chemical properties of concrete. So, dosage of SP was kept constant for all mixes. For low slump concrete mix, the secondary reaction may get delayed due to improper compaction and loss in binder content. But once the formation of $Ca(OH)_2$ starts that problem will be eased out, so the strength parameter will be dependent on one variable i.e., w/b ratio, which will not be seen if the dosage of SP is increased.

From Fig. 1, it can be seen that all slump values ranged between 80 and 130 mm except for the mixes containing a higher percentage of SF and *k* value more than 4. The results are in agreement with those reported in the literature [45]. Moreover, SF increases water demand to improve workability as it has very fine particles [50–52]. SF is considered as a highly reactive pozzolanic material which provides an increased cohesiveness in concrete due to its high fineness which consequently results into a high amount of water requirement to maintain the desired workability. Moreover. The workability of HSC decreases with the increase in the percentage of SF because the smaller particle size and higher specific surface of SF increase the water demands of concrete.

Compressive strength test results

In the present work, for different percentage of SF and the range of *k* values, compressive strength was evaluated and is presented in Table 3. At the same w/b ratio, the contribution of SF to the strength of concrete was found to be nonlinear and the increase in SF content does not necessarily lead to a proportional effect on strength. Further, at a constant w/b ratio the compressive strength of concrete decreases with an increase in *k* value. The maximum compressive strength was achieved at 6% replacement level of SF at almost all k value. Earlier work [53, 54] on SF concrete has demonstrated that the maximum compressive strength of concrete gained at 10% SF blending which can be said as the optimum dose. But a decreasing trend in compressive strength is observed when the replacement level exceeds 10%. The higher cementing efficiency of SF reduces the binder content in the mix. The formation of $Ca(OH)_2$ is fully utilized by secondary pozzolan available in the SF [55] at lower *k* value. At higher *k* value and at higher per cent replacement level of SF (> 6%), the reduction in cement content was more than 25%. Further, it is well known that natural pozzolan transforms $Ca(OH)_2$ (a hydration product of cement) to C–S–H, and when the cement content decreases hydration product will decrease, and consequently $Ca(OH)_2$ amount and the C–S–H will decrease, and hence, the compressive strength and UPV value decreases at the higher *k* value for higher percentage replacement level of SF.

UPV test results

Figure 2 shows the variation of UPV at different replacement levels of cement by SF and different *k* values. From Fig. 2,

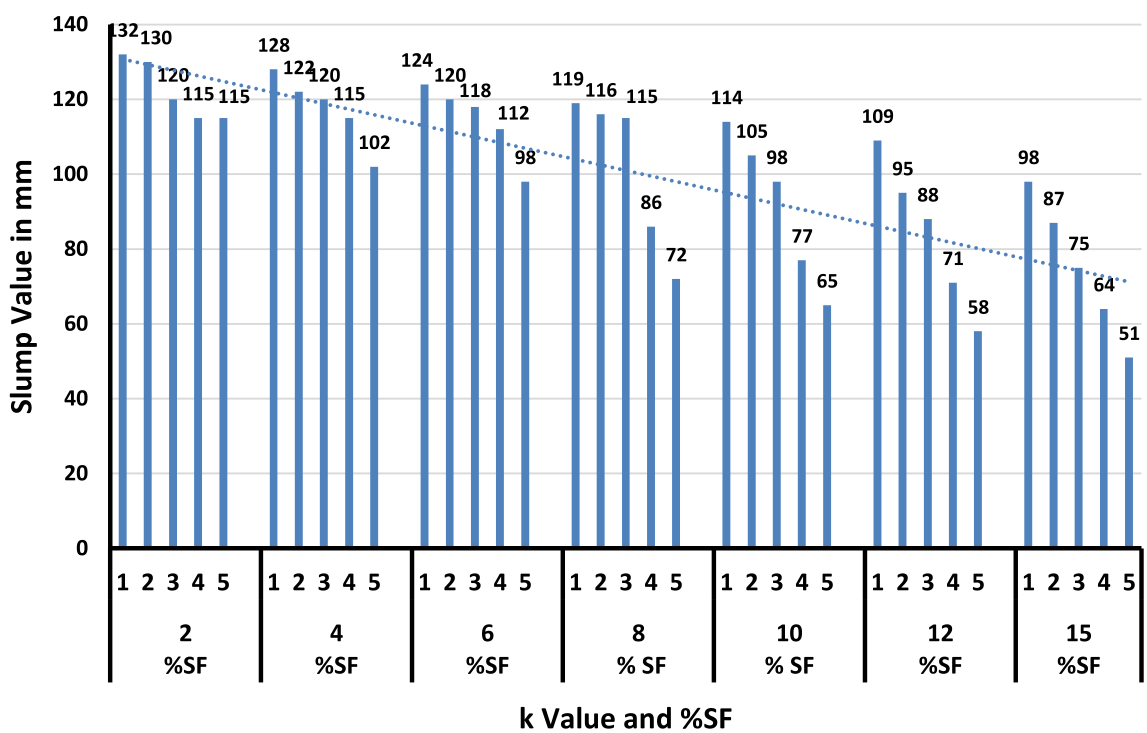

Fig. 1 Slump test results

Table 3 Compressive strength and UPV test results

%SF	Efficiency factor	Compressive strength (MPa)			UPV (28 days)
		7 Days	14 Days	28 Days	
0	–	31.21	41.43	69.04	3713
2	1	33.37	47.65	78.72	5437
4		34.78	47.88	79.01	5343
6		35.78	48.16	79.40	5322
8		34.68	47.17	76.88	4961
10		33.88	45.26	75.87	4698
12		33.12	44.38	74.03	4457
15		31.76	43.89	70.63	4100
2	2	31.67	46.32	76.31	5297
4		33.08	46.75	76.46	5260
6		34.08	47.09	76.83	5134
8		33.98	44.84	72.78	4759
10		32.18	43.27	71.42	4298
12		31.72	42.68	69.53	4126
15		30.87	41.31	66.23	3896
2	3	33.58	46.98	73.39	5045
4		34.47	47.12	73.51	5061
6		35.56	47.58	74.15	5087
8		33.03	44.16	69.11	4656
10		31.96	43.19	66.43	4254
12		31.09	42.11	64.83	3996
15		30.52	41.26	60.12	3787
2	4	33.86	47.06	70.37	4941
4		34.14	47.54	70.59	4823
6		34.98	47.92	71.12	4777
8		31.02	42.11	64.83	4326
10		29.55	41.97	60.87	4087
12		28.96	41.23	59.03	3808
15		27.83	40.67	54.55	3572
2	5	32.28	44.07	66.62	4787
4		32.88	44.42	66.93	4687
6		33.67	44.97	67.87	4694
8		28.78	40.21	59.77	4256
10		27.82	37.05	55.36	3947
12		27.08	36.62	53.82	3657
15		26.47	35.83	48.32	3298

it can be inferred that at higher k value the pulse velocity reading was on the lower side. Figure 2 also shows the linear dependency of UPV with k value. Figure 3 represents the effect of SF on pulse velocity reading of HSC. From the graph shown through Fig. 3, it can be interpreted that at a given strength, specimens with a higher SF content (8–15%) exhibit lower UPV readings than specimens with a lower SF content (2–6%). This indicates that the mixture with a lower SF content is denser than the mixture with a higher SF content at the same k value.

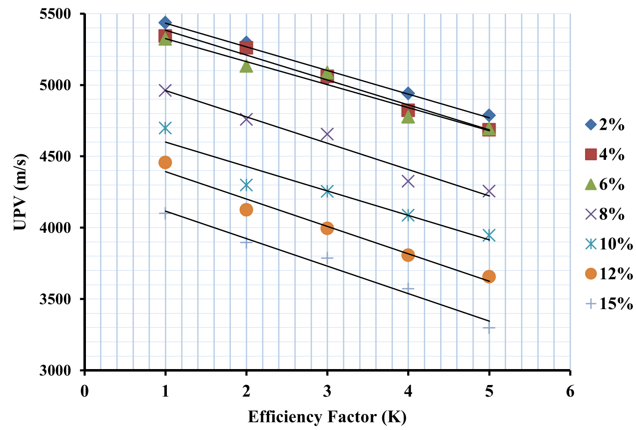

Fig. 2 Variation of UPV at different k values

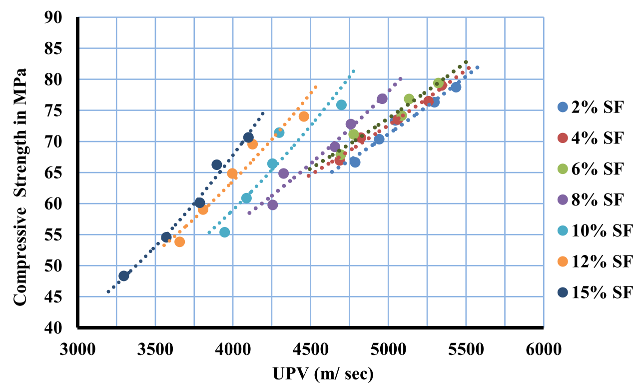

Fig. 3 Effect of SF on pulse velocity reading

Owing to the deflocculating of the cement grain, the capability of the SF particles to insert themselves between the cement grains had contributed to water reduction. As the percentage replacement level of SF increases (8–15%), the more surface area of the SF needs to be wetted; thus, the demand for water increases. A large amount of SF is left un-dispersed evenly and uniformly, creating a lesser dense material. That explained the lower UPV reading in mixture with a high percentage (> 8%) of SF compared to mixtures with < 8% SF.

Correlation study and model development

Correlation between compressive strength and efficiency factor for SF

A fundamental rule of concrete technology is that a distinctive relationship between the w/c-ratio and strength occurs for a given material. When SF is introduced, this relationship is modified quantitatively, but not qualitatively. From Fig. 4, it is noted that the curves for k versus compressive

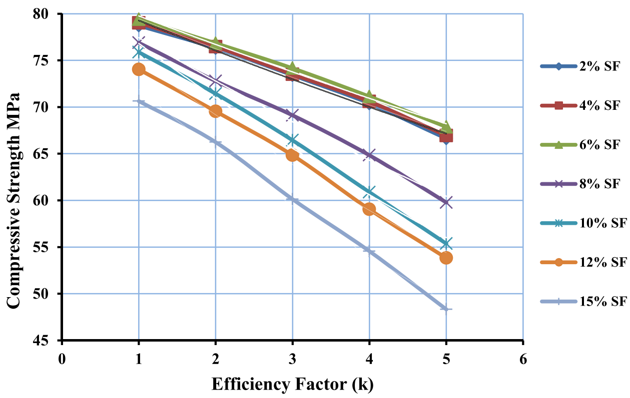

Fig. 4 Efficiency factor versus compressive strength

strength are similar to the curves of w/c versus compressive strength. Both curves can be approximated by an exponential function similar to that introduced by Abram's. Using a fixed w/b ratio increase in the percentage of SF results in a shift in the strength versus *k* curve, but the shape of the curve is maintained.

Processing data points on any of the curves through Microsoft Excel gives a simple empirical function and can be written as a function of *k* factor. The relation between concrete compressive strength and *k* value for SF can be generalized in the form similar to that of Abram's law as presented in Eq. 2. In Eq. 2, f_{ck} signifies the 28-day cube compressive strength in MPa.

$$f_{ck} = \alpha_1 \cdot e^{\beta_1 \cdot k} \tag{2}$$

The values of the constant α_1 and β_1 corresponding to each % of SF are presented in Table 4.

Correlation between compressive strength and UPV

For the prediction of f_{ck}, several researchers [39, 56–61] have proposed regression model between f_{ck} and UPV. An exponential relationship has been reported in the literature [62–67], between UPV and f_{ck}, while few other studies [57, 58, 68] on correlation between UPV and f_{ck} reported power product equation. The most popular being the exponential relationship which can be abridged by Eq. 3.

$$f_{ck} = \alpha_2 \cdot e^{\beta_2 \cdot V_p} \tag{3}$$

where f_{ck} is compressive strength in MPa; V_p is UPV in m/s; α_2 and β_2 are regression coefficients.

From Fig. 5, it can be observed that the rate of increase in pulse velocity was identical at all *k* values, as a single trend line was obtained for all percentage replacement of OPC with SF. A good correlation in terms of exponential function was observed between UPV and f_{ck}, as can be seen from Fig. 5 and Eq. 4.

$$f_{ck} = 27.87 \cdot e^{0.000198 \cdot V_p} \tag{4}$$

where $\alpha_2 = 27.87$ and $\beta_2 = 0.000198$.

The predicted f_{ck} obtained through Eq. 4 were compared with experimental values of f_{ck} from this research and is shown in Fig. 6. Further, to validate the accuracy of the formula suggested in this study, the test-to-predicted ratio of concrete compressive strength from the recommended equation were compared with those of other proposed equations developed for UPV and f_{ck} as summarized in Table 5. The predicted compressive strength from the proposed equation by other authors were obtained from the UPV values obtained in this research. The results demonstrate that the vast majority of the considered equations overestimate the compressive strength of HSC, while the proposed Eq. 4 underestimates the compressive strength when compared with the results of other authors.

Response surface regression: UPV versus %SF, *k*

A detailed analysis of variance (ANOVA) was conducted to assess the influence of the variables (%SF and *k*) on UPV results. The influence of the interaction among the variables on UPV results was also assessed through ANOVA. In the

Table 4 Constants corresponding to %SF

α_1	β_1	%SF
82.624	−0.0415	2
82.796	−0.0412	4
82.942	−0.0391	6
82.3747	−0.0619	8
83.1228	−0.079	10
81.1863	−0.0801	12
79.1029	−0.0953	15

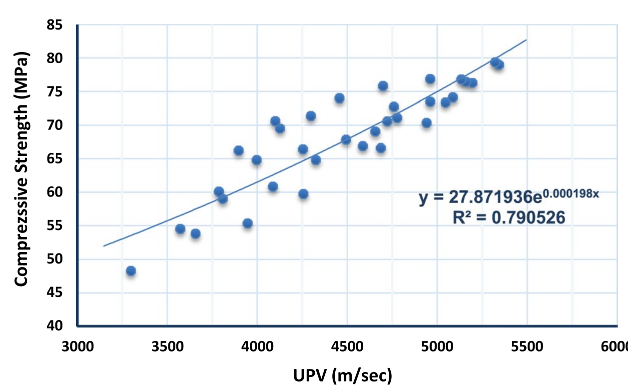

Fig. 5 UPV versus compressive strength

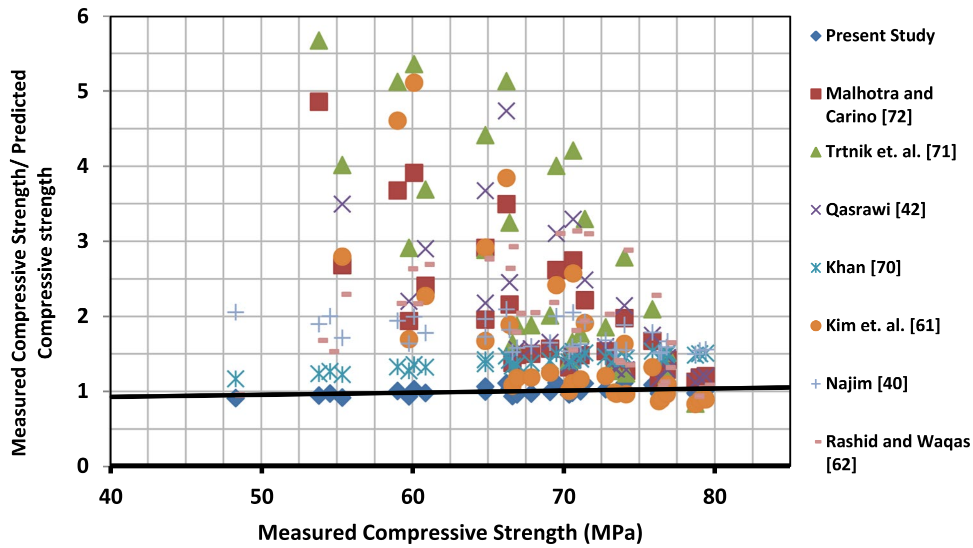

Fig. 6 Experimental versus predicted compressive strength

Table 5 Proposed equations developed for UPV and compressive strength

References	Regression formula (MPa)	Expression types
Khan [69]	$f_{ck} = \left(0.5208V_p\right)^5$	Power
Kim et al. [60]	$f_{ck} = 50.163V_p - 178.2$	1st polynomial
Najim [39]	$f_{ck} = 0.0136V_p - 21.34$	1st polynomial
Qasrawi [41]	$f_{ck} = 36.72V_p - 129.077$	1st polynomial
Trtnik et al. [70]	$f_{ck} = 0.854e^{1.2882V_p}$	Exponential
Malhotra and Carino [71]	$f_{ck} = 109.6 + \left(0.33 \times V_p\right)$	Linear
Rashid and Waqas [61]	$f_{ck} = 38.05V_p^2 - 316.76V_p + 681.62$	2nd polynomial
Present Work	$f_{ck} = 27.87e^{0.000198V_p}$	Exponential

Table 6 Analysis of variance

Source	DF	Adj SS	Adj MS	*F* Value	*P* Value
Model	5	10,855,092	2,171,018	153.88	0.000
Linear	2	10,814,313	5,407,156	383.26	0.000
%SF	1	8,607,478	8,607,478	610.10	0.000
k	1	2,206,834	2,206,834	156.42	0.000
Square	2	83,152	83,152	2.95	0.068
%SF×%SF	1	81,419	81,419	5.77	0.023
k×*k*	1	1732	1732	0.12	0.729
2-Way interaction	1	5674	5674	0.40	0.531
%SF×k	1	5674	5674	0.40	0.531
Error	29	409,141	14,108		
Total	34	11,264,232			

present analysis, ANOVA of the test results was performed using the MINITAB programme.

The first column (Table 6) defines the cause of variance, and the second column specifies the degrees of freedom (DF) defined for each particular event. In general, the DF is the measure of how much "independent" information is available to calculate each sum of squares (SS). The DF (Regression) is one less than the number of parameters being estimated. There are k predictor variables and so there are *k* parameters for the coefficients on those variables. There is always one additional parameter for the constant, so there are $k+1$ parameters. But the DF is one less than the number of parameters, so there are $k+1-1=k$ degrees of freedom. Hence, the DF is equal to 1 as we have only one output parameter. Adj SS is the sum of the squared differences between the observed (experimental data set of the response variable) and the mean value of the response variable, while Adj MS is the mean squares which are the sum of the squares divided by degree of freedom. The *F* value corresponds to the ratio of the related mean squares to the overall mean square due to error, whereas the *P* value is the interval of confidence in which the test method changes conclusions. A confidence interval (CI) is an interval used to estimate a response from the data available from research. The CI is a range of values that's likely to include a response value with a certain degree of confidence. It is often expressed as a per cent. Based on ANOVA, both the linear terms (%SF and *k*) were statistically significant at 95% CI; further, the square term $k \times k$ and the interaction term $SF \times k$ was removed from the response surface regression model as the P value was 0.729 and 0.531, respectively, and was not statistically significant.

The experimental data are used in the model through response surface regression which consisted of the terms which are statistically significant at a 0.05 level. Quadratic interactions were made to obtain the regression equations. A statistically noteworthy model with a high correlation coefficient $R^2 > 0.90$ was established and is presented through Eq. 5.

$$V_p = 5863.0 - 67.9 \times (\%SF) - 177.4 \times k - 2.92 \times (\%SF)^2 \quad (5)$$

Table 7 summarizes the model equation obtained through response surface regression. Predicted R^2 is more helpful than adjusted R^2 for comparing models since it is computed with observations excluded in the model calculation.

S, R^2, adjusted R^2, and predicted R^2 are measurements of how well the model matches the results. S is measured in the response variable units and represents the normal distance from the regression line that the data values fall. R^2 (R-Sq) defines the amount of variance that is described by the predictor(s) in the observed response values. Adjusted R^2 is a modified R^2 that has been adjusted for the number of terms in the model. Adjusted R^2 is used to compare models with different numbers of predictors. R^2 (pred) is a measure of how well the model predicts the response for new observations.

Table 7 Model summary

S	R-sq	R-sq(adj)	R-sq(pred)
115.918	96.30%	95.94%	95.46%

The exactness of the proposed model can be determined by comparing anticipated with measured qualities acquired with mixes prepared at the focal point of the exploratory area. In the present work, to evaluate the precision of the proposed model normal probability plot of the residuals or the error terms has been plotted. The normal probability plots shown in Fig. 7 indicate good accuracy for the established models. A probability plot graphs each value versus the percentage of values in the sample that are less than or equal to it, along a fitted distribution line. The y-axis is transformed so that the fitted distribution forms a straight line. Difference between observed value and fitted value is known as residual. The fitted value is the predicted UPV value computed using regression model. Whereas observation order is the number of data used to develop the regression model. In the histogram shown in Fig. 7, the frequency (or absolute frequency) of an event is the number of times the observation occurred in an experiment. Figure 8 shows the measured vs predicted graph of UPV.

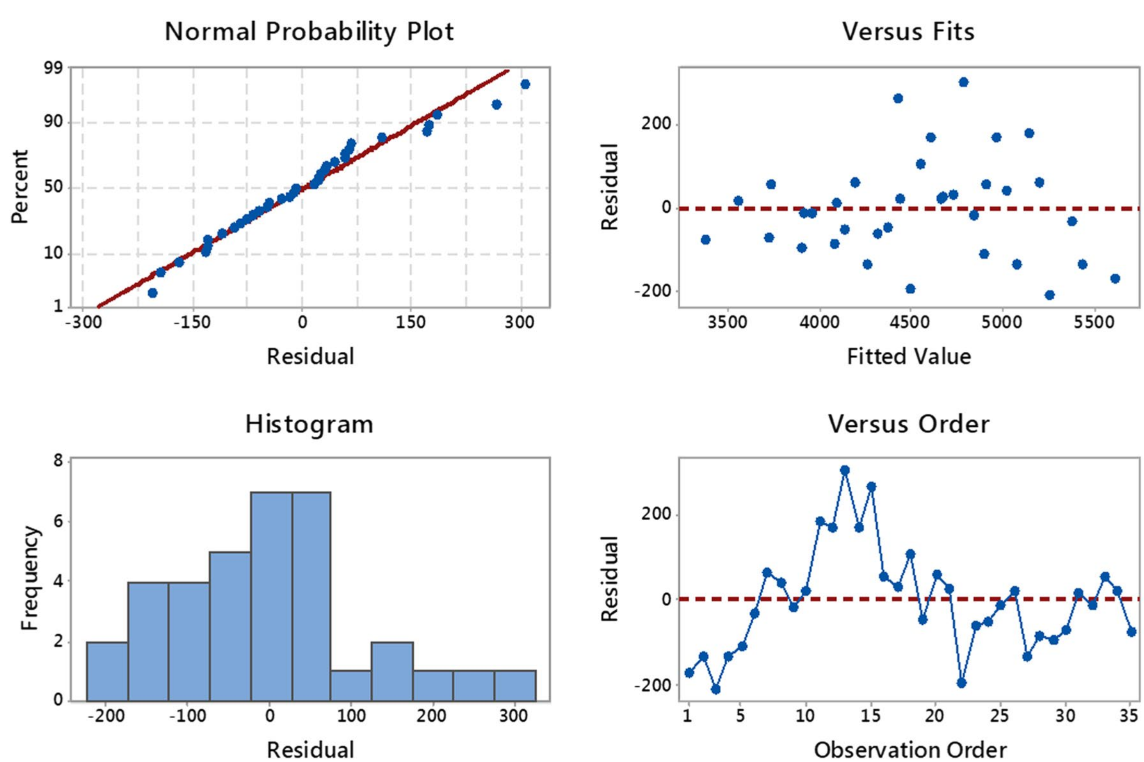

Fig. 7 Residual plots for UPV

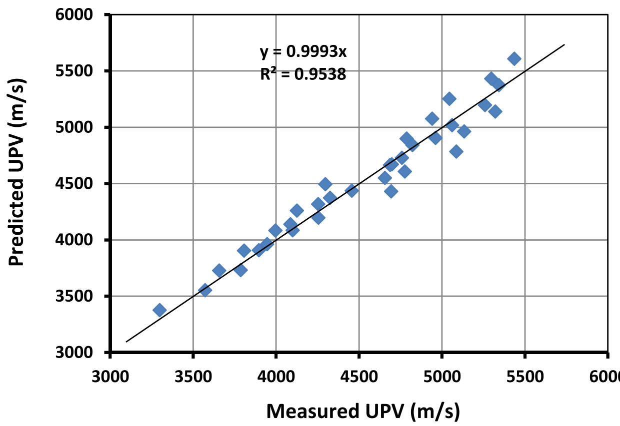

Fig. 8 Measured versus predicted values for UPV

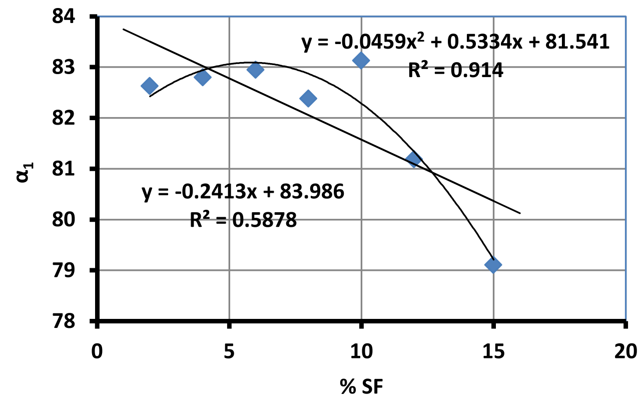

Fig. 9 Dependency of the coefficient α_1 with %SF

Strength-based model to predict compressive strength of HSC with SF

The proposed correlation discussed in the previous subsection is now effectively utilized to access the compressive strength of HSC. Further, to validate the proposed strength-based model from the database of other studies, it was necessary to correlate UPV with %SF and its k factor. All the proposed analytical formulas are incorporated in the strength-based model to predict the compressive strength of HSC in terms of k factor and %SF. Both the exponential functions proposed through Eqs. 2 and 3 were multiplied to give the following general Eq. 6:

$$f_{ck}^2 = \alpha_1 \cdot \alpha_2 \cdot e^{\beta_1 \cdot k + \beta_2 \cdot V_p} \quad (6)$$

By taking the log, Eq. 8 can be transformed into a linear function as

$$2\log_e f_{ck} = \log_e\left(\alpha_1\alpha_2\right) + \beta_1 \cdot k + \beta_2 \cdot V_p \quad (7)$$

$$\log_e f_{ck} = \left[\frac{\log_e\left(\alpha_1\alpha_2\right) + \beta_1 \cdot k + \beta_2 \cdot V_p}{2}\right] \quad (8)$$

From Fig. 2 and Table 4, it can be observed that coefficient α_1 and β_1 are dependent on %SF. Figures 9 and 10 show the dependency of the coefficients α_1 and β_1 with %SF. Here a straight line fit seems to be preferable over parabolic fit on account of similarity and simplicity and also on account of linear dependence of the UPV values with respect to k factor (Fig. 2). Thus the two constant can be expressed as

$$\alpha_1 = -0.2413 \times \%SF + 83.986 \quad (9)$$

$$\beta_1 = -0.0047 \times \%SF - 0.024 \quad (10)$$

Substituting for α_1, α_2, β_1 and β_2 in Eq. 8, the proposed compressive strength-based model equation can be represented as given by Eq. (8) where the dependent variable is a linear equation of more than an independent variable.

$$\log_e f_{ck} = \left[\frac{\log_e(27.87 \times (-0.2413 \times \%SF + 83.986)) - (0.0047 \times \%SF + 0.024) \times k + 0.000190 \times V_p}{2}\right] \quad (11)$$

Figure 11 presents the comparison of measured versus predicted compressive strength, which was obtained from Eq. 11.

Substituting for V_p (Eq. 11) in Eq. 10, the proposed compressive strength model can be modified as Eq. 12.

$$\log_e f_{ck} = \left[\frac{\log_e(2340.69 - 6.725 \times \%SF) - (0.0047 \times \%SF + 0.024) \times k + 0.00019 \times \left(5863 - 67.9 \times \%SF - 177.4 \times k - 2.92 \times (\%SF)^2\right)}{2}\right] \quad (12)$$

Taking antilog Eq. 12 can be modified in a more general form. Equation 13 presents the modified form.

$$f_{ck} = e^{\left[\frac{\log_e(2340.69 - 6.725 \times \%SF) - (0.0047 \times \%SF + 0.024) \times k + 0.00019 \times \left(5863 - 67.9 \times (\%SF) - 177.4 \times k - 2.92 \times (\%SF)^2\right)}{2}\right]} \quad (13)$$

The applicability of the proposed equation is verified from the data set of authors whose k values were known and is shown in Table 8. The percentage error presented in Table 8 clearly shows that the database of other researchers'

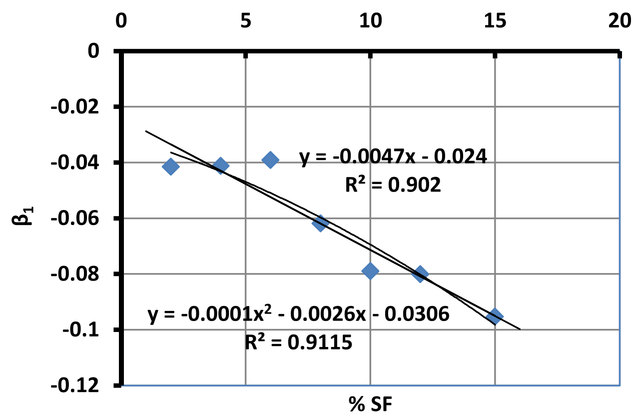

Fig. 10 Dependency of the coefficient β_1 with %SF

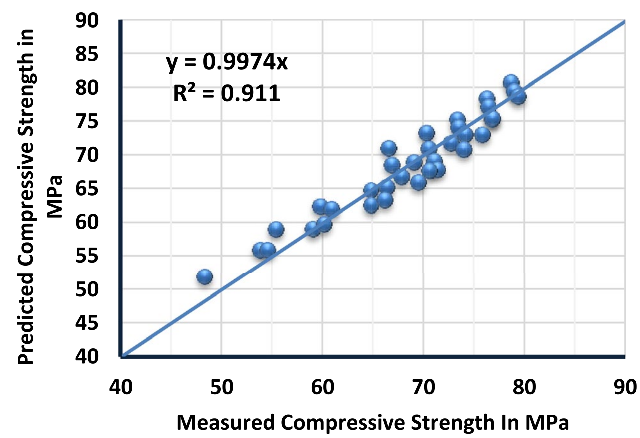

Fig. 11 Measured versus predicted compressive strength

Table 8 Validation of proposed strength-based model from the database of other authors

Authors	w/b	%SF	*k*	Compressive strength (MPa) 28 Days	Predicted compressive strength (MPa)	% Error
Malathy and Subramanian [28]	0.30	2.5	2.15	75.28	78.35	3.91
		5	2.61	75.56	73.97	−2.15
		7.5	2.75	78.67	70.26	−11.97
		10	2.93	82.76	66.24	−24.93
	0.35	2.5	2.15	62.63	78.35	20.06
		5	2.61	65.55	73.97	11.38
		7.5	2.75	68.42	70.26	2.62
		10	2.93	72.13	66.24	−8.88
Bhanja and Sengupta [14]	0.34	5	6.83	64.3	62.13	−3.49
		10	5.33	72.0	58.32	−23.45
	0.38	5	6.83	60.2	62.13	3.11
		10	5.33	66.5	58.32	−14.02
		15	4.06	67.6	55.06	−22.77
	0.42	10	5.33	57.5	58.32	1.41
		15	4.06	60.7	55.06	−10.24
		20	3.01	62.7	51.91	−20.80
Maage [13]	0.64	5	6.83	50.1	62.13	19.37
	0.70	10	5.33	53.6	58.32	8.10
Sorensen [72]	0.38	10	5.33	63.7	58.32	−9.22
		20	3.01	53.3	51.91	−2.69
	0.40	20	3.01	50.0	51.91	3.67
	0.37	10	5.33	56.2	58.32	3.64
Yamato and Emoto [73]	0.35	5	8.89	62.1	57.07	−8.82
		10	5.73	64.3	57.10	−12.61
	0.45	5	7.40	49.0	60.69	19.26
		10	6.98	57.3	53.43	−7.23
		20	3.01	52.70	51.31	−2.70
	0.25	10	2.64	68.3	67.27	−1.53

lies within ± 15% to ± 20% limits, which verifies the applicability of the model. The proposed model is for the strength range of the 40–75 MPa.

Conclusions

Considerable numbers of experiments were performed on high-strength concrete (HSC) to determine the isolated influence of silica fume (SF) on the efficiency factor (*k*) on compressive strength and ultrasonic pulse velocity (UPV) of concrete over a wide range of *k* values varying from 1 to 5 and SF replacement percentages ranging from 2 to 15. The following conclusions could be derived from the exploratory research programme.

1. Workability of HSC mixes with SF follows a decreasing trend with increasing SF content. However, at the optimum dosage of SF (6%), minimum slump of 98 mm was obtained which was quite satisfactory and was beyond the desired range.
2. The desired value of strength (60 MPa) was achieved at 6% replacement of SF with a *k* value of 4.
3. For *k* value up to 4 and SF replacement up to 6% led to reduction in cement content by 24%. At higher *k* value, increase in SF content in HSC mixes decreases the compressive strength and UPV value due to the unutilized pozzolana reduces the compressive strength and UPV values.
4. The *k* value can be used to transform a certain amount of pozzolan to an equivalent amount of cement in terms of strength contribution; hence, it can be used as a basis for more efficient proportioning of blended concrete.
5. A prediction formula for evaluating compressive strength from UPV values has been proposed. A very good agreement between the experimental and predicted compressive strength was observed.
6. The present work also proposed a new model to predict the 28 days compressive strength of concrete based on UPV, %SF, and *k* value. The prediction of concrete compressive strength with the proposed numerical model demonstrated a decent level of coherency with experimentally evaluated compressive strength.
7. Concrete strength depends upon the molecular arrangement of its hydrated constituents compounds. The UPV value is used as an indicator of the microstructure development of concrete. In young concrete, with the progress of hydration, the solid phase in the system becomes more connected. In the present work, the UPV measurement and compressive strength, directly or indirectly, reveal the development of microstructure during and after the cement hydration process. The ease of passing ultrasonic waves through the concrete samples indirectly indicates the formation of dense microstructure and thus indicating the reduction of voids in the concrete matrix. The modelled equation elucidates this effect as the influence of %SF and its cementing efficiency factor on UPV have been incorporated in the proposed model equation.
8. The validity of the model has been verified with the results obtained by different researchers on different types of specimens. The proposed model is for the strength range of the 40–75 MPa. This model enables us to effectively and dependably estimate the compressive strength of silica fume concrete.

This study may have limitations as various influencing factors, like aggregate conditions and admixture replacement, were not considered to improve the reliability of the proposed model. Further, it is recommended that testing of concrete produced with SF extended to 60 or 90 days to further determine the pozzolanic effect of SF in terms of durability properties.

Compliance with ethical standards

Conflict of interest On behalf of all authors, the corresponding author states that there is no conflict of interest.

References

1. ACI Committee 318 (1995) Building code requirements for structural concrete (ACI 318-95) and commentary (ACI 318R-95). Am Concr Inst 552:503
2. C. CEB-FIP, Model Code 1990, Com. Euro-International Du Beton, Paris. (1991) 87–109. https://doi.org/10.1680/ceb-fipmc1990.35430
3. Shen D, Wen C, Zhu P, Wu Y, Yuan J (2020) Influence of Barchip fiber on early-age autogenous shrinkage of high strength concrete. Constr Build Mater. https://doi.org/10.1016/j.conbuildmat.2020.119223
4. Shen D, Li C, Feng Z, Wen C, Ojha B (2019) Influence of strain rate on bond behavior of concrete members reinforced with basalt fiber-reinforced polymer rebars. Constr Build Mater. https://doi.org/10.1016/j.conbuildmat.2019.116755
5. Shen D, Wen C, Zhu P, Li M, Ojha B, Li C (2020) Bond behavior between basalt fiber-reinforced polymer bars and concrete under cyclic loading. Constr Build Mater. https://doi.org/10.1016/j.conbuildmat.2020.119518
6. Villar-Cociña E, Rodier L, Savastano H, Lefrán M, Rojas MF (2020) A comparative study on the Pozzolanic activity between bamboo leaves ash and silica fume: kinetic parameters. Waste Biomass Valorization 1–8. https://doi.org/10.1007/s12649-018-00556-y
7. Sharaky IA, Megahed FA, Seleem MH, Badawy AM (2019) The influence of silica fume, nano silica and mixing method on the strength and durability of concrete. SN Appl Sci 6:575–584. https://doi.org/10.1007/s42452-019-0621-2
8. Güneyisi E, Gesoğlu M, Karaoğlu S, Mermerdaş K (2012) Strength, permeability and shrinkage cracking of silica fume and metakaolin concretes. Constr Build Mater 34:120–130. https://doi.org/10.1016/j.conbuildmat.2012.02.017

9. Siddique R, Khan MI (2011) Supplementary cementing materials. In: Springer Sci. Business, Media, pp 67–120
10. Wang F, Li S (2012) Effect of silica fume on workability and water impermeability of concrete. Appl Mech Mater 238:157–160. https://doi.org/10.4028/www.scientific.net/AMM.238.157
11. Mohan A, Mini KM (2018) Strength and durability studies of SCC incorporating silica fume and ultra fine GGBS. Constr Build Mater 171:919–928. https://doi.org/10.1016/j.conbuildmat.2018.03.186
12. Khayat KH, Yahia A, Sayed M (2008) Effect of supplementary cementitious materials on rheological properties, bleeding, and strength of structural grout. ACI Mater J 35:842–849. https://doi.org/10.14359/20200
13. Maage M (1989) Efficiency factors for condensed silica fume in concrete. ACI Spec Publ 114:783–798
14. Bhanja S, Sengupta B (2002) Investigations on the compressive strength of silica fume concrete using statistical methods. Cem Concr Res 32:1391–1394. https://doi.org/10.1016/S0008-8846(02)00787-1
15. Albattat RAI, Jamshidzadeh Z, Alasadi AKR (2020) Assessment of compressive strength and durability of silica fume-based concrete in acidic environment. Innov Infrastruct Solut 5:20. https://doi.org/10.1007/s41062-020-0269-1
16. Smith IA (1967) The design of fly ash concretes. Proc Inst Civ Eng 36:769–790. https://doi.org/10.1680/iicep.1967.8472
17. Jahren P (1983) Use of silica fume in concrete. ACI Spec Publ 79:677–694. https://doi.org/10.14359/6715
18. Sellevold EJ, Radjy FF (1983) Condensed silica fume (Microsilica) in concrete: water demand and strength development. Spec Publ 79:677–694
19. Gopalan MK, Hague MN (1985) Design of flyash concrete. Cem Concr Res 15:694–702. https://doi.org/10.1016/0008-8846(85)90071-7
20. Babu KG, Rao GSN (1993) Efficiency of fly ash in concrete. Cem Concr Compos 15:223–229. https://doi.org/10.1016/0958-9465(93)90025-5
21. Feret R (1892) On the compactness of hydraulic mortars. Memoirs and documents relating to the art of constructions at the service of the engineer. Ann Des Ponts Chaussées. 2nd semest 5–161
22. Bolomy (1927) Durcissemenr des morriers er betons. Bull Tech Suisse Rom 16–24
23. Abrams DA (1918) Design of Concrete Mixtures, Bull. No. 1, Struct. Mater. Lab. Lewis Institute, Chicago, p 20
24. Slanička Š (1991) The influence of condensed silica fume on the concrete strength. Cem Concr Res 21:462–470. https://doi.org/10.1016/0008-8846(91)90094-X
25. Ganesh Babu K, Surya Prakash PV (1995) Efficiency of silica fume in concrete. Cem Concr Res 25:1273–1283. https://doi.org/10.1016/0008-8846(95)00120-2
26. Loland K (1981) Silica concrete (Norwegian). In: J Nord Concr Fed
27. Fagerlund G (1981) Definition of water/cement ratio using silica fume Swedish. In: Intern. Cem Rep
28. Malathy R, Subramanian K (2007) Efficiency factor for silica fume & metakaoline at various replacement levels. Singapore Concr Inst (2007). http://cipremier.com/100032037%5Cnwww.cipremier.com
29. Yoshitake I, Inoue S, Miyamoto K (2019) Strength properties of durable concrete made with various alternative. Interdepend Between Struct Eng Constr Manag 1–6
30. Khan AN, Magar RB, Chore HS (2018) Efficiency factor of supplementary cementitious materials: a state of art. Int J Optim Civ Eng 8:247–253
31. Li LG, Zheng JY, Ng PL, Zhu J, Kwan AKH (2019) Cementing efficiencies and synergistic roles of silica fume and nano-silica in sulphate and chloride resistance of concrete. Constr Build Mater 223:965–975. https://doi.org/10.1016/j.conbuildmat.2019.07.241
32. Sharaky IA, Megahed FA, Seleem MH, Badawy AM (2019) The influence of silica fume, nano silica and mixing method on the strength and durability of concrete. SN Appl Sci 1:1–10. https://doi.org/10.1007/s42452-019-0621-2
33. Pereira N, Romão X (2016) Material strength safety factors for the seismic safety assessment of existing RC buildings. Constr Build Mater 119:319–328. https://doi.org/10.1016/j.conbuildmat.2016.05.055
34. Breysse D (2012) Nondestructive evaluation of concrete strength: an historical review and a new perspective by combining NDT methods. Constr Build Mater. https://doi.org/10.1016/j.conbuildmat.2011.12.103
35. Lin Y, Lai CP, Yen T (2003) Prediction of ultrasonic pulse velocity (UPV) in concrete. ACI Mater J 100:21–28. https://doi.org/10.14359/12459
36. Ju M, Park K, Oh H (2017) Estimation of compressive strength of high strength concrete using non-destructive technique and concrete core strength. Appl Sci. https://doi.org/10.3390/app7121249
37. Khan SRM, Noorzaei J, Kadir MRA, Waleed AMT, Jaafar MS (2007) UPV method for strength detection of high performance concrete. Struct Surv 25:61–73
38. Atici U (2011) Prediction of the strength of mineral admixture concrete using multivariable regression analysis and an artificial neural network. Expert Syst Appl. https://doi.org/10.1016/j.eswa.2011.01.156
39. Najim KB (2017) Strength evaluation of concrete structures using ISonReb linear regression models: laboratory and site (case studies) validation. Constr Build Mater 149:639–647. https://doi.org/10.1016/j.conbuildmat.2017.04.162
40. Atahan HN, Oktar ON, Tademir MA (2011) Factors determining the correlations between high strength concrete properties. Constr Build Mater. https://doi.org/10.1016/j.conbuildmat.2010.11.005
41. Qasrawi HY (2000) Concrete strength by combined nondestructive methods simply and reliably predicted. Cem Concr Res. https://doi.org/10.1016/S0008-8846(00)00226-X
42. IS: 8112 (1989) Ordinary Portland cement, 43 grade-Specification. Bur. Indian Stand., New Delhi
43. IS:383 (2016) Specification for coarse and fine aggregates from natural sources for concrete. Bur. Indian Stand., New Delhi, India, pp 1–18
44. IS:516 (2004) Method of tests for strength of concrete. Bur. Indian Stand., New Delhi, India
45. Biswas R, Rai B (2020) Effect of cementing efficiency factor on the mechanical properties of concrete incorporating silica fume. J Struct Integr Maint 5:190–203. https://doi.org/10.1080/24705314.2020.1765269
46. IS:10262, IS:10262-2009 (2009) Indian standards recommended Guidelines for concrete mix design. In: Bur. Indian Stand., New Delhi, India
47. IS: 1199 (1959) Methods of sampling and analysis of concrete. Bur. Indian Stand., New Delhi
48. IS: 516 (1959) Method of test for strength of concrete. Bur. Indian Stand., New Delhi
49. IS:13311 (Part-1) (1992) Non-destructuctive testing of concrete-method of testing. Bur. Indian Stand., New Delhi
50. Khatri RP, Sirivivatnanon V, Gross W (1995) Effect of different supplementary cementitious materials on mechanical properties of high performance concrete. Cem Concr Res 25:209–220. https://doi.org/10.1016/0008-8846(94)00128-L
51. Mazloom M, Ramezanianpour AA, Brooks JJ (2004) Effect of silica fume on mechanical properties of high-strength concrete. Cem Concr Compos. https://doi.org/10.1016/S0958-9465(03)00017-9

52. Kovler K, Roussel N (2011) Properties of fresh and hardened concrete. Cem Concr Res. https://doi.org/10.1016/j.cemconres.2011.03.009
53. Behnood A, Ziari H (2008) Effects of silica fume addition and water to cement ratio on the properties of high-strength concrete after exposure to high temperatures. Cem Concr Compos. https://doi.org/10.1016/j.cemconcomp.2007.06.003
54. Ismeik M (2009) Effect of mineral admixtures on mechanical properties of high strength concrete made with locally available materials. Jordan J. Civ, Eng
55. Kadri EH, Duval R (2009) Hydration heat kinetics of concrete with silica fume. Constr Build Mater. https://doi.org/10.1016/j.conbuildmat.2009.06.008
56. Kashiyani BK, Pitroda J, Shah DBK (2012) A study of utilization aspect of polypropylene fibre for making value added concrete. Int J Sci Res 2:103–106. https://doi.org/10.15373/22778179/feb2013/37
57. Alwash M, Breysse D, Sbartaï ZM (2015) Non-destructive strength evaluation of concrete: analysis of some key factors using synthetic simulations. Constr Build Mater. https://doi.org/10.1016/j.conbuildmat.2015.09.023
58. Alwash M, Sbartaï ZM, Breysse D (2016) Non-destructive assessment of both mean strength and variability of concrete: a new bi-objective approach. Constr Build Mater. https://doi.org/10.1016/j.conbuildmat.2016.03.120
59. A.I. of Japan (1983) Manual of nondestructive test methods for the evaluation of concrete strength. In: Archit. Inst. Japan Tokyo, Japan
60. Kim WM, Oh H, Oh KC (2016) Estimating the compressive strength of high-strength concrete using surface rebound value and ultrasonic velocity. J Korea Inst Struct Maint Insp 20:1–9. https://doi.org/10.11112/jksmi.2016.20.2.001
61. Rashid K, Waqas R (2017) Compressive strength evaluation by non-destructive techniques: an automated approach in construction industry. J Build Eng 12:147–154. https://doi.org/10.1016/j.jobe.2017.05.010
62. Bungey J (1984) The use of ultrasonics for NDT of concrete. In: Brit J NDT, pp 366–369
63. Galan A (1990) Combined ultrasound methods of concrete testing. In: North-Holland, Elsevier, Amsterdam
64. Ismail M, Yusof K, Ibrahim A (1996) A combined ultrasonic method on the estimation of compressive concrete strength. INSIGHT 38:781–785
65. Pascale GP, Di Leo A, Carli R (2000) Evaluation of actual compressive strength of high strength concrete by NDT. 15th World conf. non-destructive test, 10p. https://www.ndt.net/article/wcndt00/papers/idn527/idn527.htm
66. Atici U (2010) Prediction of the strength of mineral-addition concrete using regression analysis. Mag Concr Res 62:585–592. https://doi.org/10.1680/macr.2010.62.8.585
67. Del Río LM, Jiménez A, López F, Rosa FJ, Rufo MM, Paniagua JM (2004) Characterization and hardening of concrete with ultrasonic testing. Ultrasonics 42:527–530. https://doi.org/10.1016/j.ultras.2004.01.053
68. Mohammed BS, Azmi NJ, Abdullahi M (2011) Evaluation of rubbercrete based on ultrasonic pulse velocity and rebound hammer tests. Constr Build Mater. https://doi.org/10.1016/j.conbuildmat.2010.09.004
69. Khan MI (2012) Evaluation of non-destructive testing of high strength concrete incorporating supplementary cementitious composites. Resour Conserv Recycl 61:125–129. https://doi.org/10.1016/j.resconrec.2012.01.013
70. Trtnik G, Kavčič F, Turk G (2009) Prediction of concrete strength using ultrasonic pulse velocity and artificial neural networks. Ultrasonics 49:53–60. https://doi.org/10.1016/j.ultras.2008.05.001
71. Malhotra V, Carino N (2010) Handbook on nondestructive testing of concrete, 2nd ed. https://doi.org/10.1201/9781420040050
72. Sorensen EV (1983) Freezing and thawing resistance of condensed silica fume (Microsilica) concrete exposed to deicing chemicals. ACI Spec Publ 79:709–718. https://www.concrete.org/publications/internationalconcreteabstractsportal.aspx?m=details&i=6720
73. Yamato T, Emoto Y (1989) Chemical resistance of concrete containing condensed silica fume. Spec Publ 114:897–914